Biosensors and Bioelectronics 85 (2016) 897–902

Contents lists available at ScienceDirect

Biosensors and Bioelectronics

journal homepage: www.elsevier.com/locate/bios

MicroRNA-mediated signal amplification coupled with GNP/dendrimers on a mass-sensitive biosensor and its applications in intracellular microRNA quantification

Yingshu Guo [a,b], Yujie Wang [b,c], Guangxu Yang [d], Jing-Juan Xu [a,*], Hong-Yuan Chen [a]

[a] State Key Laboratory of Analytical Chemistry for Life Science and Collaborative Innovation Center of Chemistry for Life Sciences, School of Chemistry and Chemical Engineering, Nanjing University, Nanjing 210023, China
[b] Shandong Province Key Laboratory of Detection Technology for Tumor Makers, School of Chemistry and Chemical Engineering, Linyi University, Linyi 276005, China
[c] College of Chemistry, Chemical Engineering and Materials Science, Collaborative Innovation Center of Functionalized Probes for Chemical Imaging in Universities of Shandong, Key Laboratory of Molecular and Nano Probes, Ministry of Education, Shandong Normal University, Jinan 250014, China
[d] Key Laboratory of Biochemical Analysis, Ministry of Education, College of Chemistry and Molecular Engineering, Qingdao University of Science and Technology, Qingdao 266042, China

ARTICLE INFO

Article history:
Received 7 March 2016
Received in revised form
6 June 2016
Accepted 6 June 2016

Keywords:
MicroRNA
Cell
Quartz crystal microbalance
Dendrimer

ABSTRACT

Here, a mass-sensitive microRNA sensing surface is developed by utilizing a probe DNA/gold nanoparticles (GNP)/dendrimer composite coupling with an enzymatic amplification process. The probe DNA/GNP/dendrimer composite is prepared via the covalent coupling between the NH_2 groups in PAMAM or DNA and the COOH group on GNP. Target microRNA binds to a stem-loop-structured DNA on maganatic NPs, forming a heteroduplex. By enzyme recycling amplification, a large number of linker sequences are produced on MNPs. Via the combination of probe DNA, the linker DNA on MNPs and a capture DNA on gold chip, the DNA/GNP/dendrimer probe could be assembled on the surface of gold chip inducing a sensitive frequency response. It presents an excellent performance in microRNA-203 quantification with a detection linear range of 1.0×10^{-11}–1.0×10^{-9} M. Both the success in discriminating expressing miroRNA-203 in MCF-7 cell and the well agreement with the commercial qRT-PCR detection method implied its potential application in early cancer diagnosis for future.

1. Introduction

MicroRNA (miRNA) is a group of endogenous, single-strand non-coding ribonucleic acid molecules with a typical length of ~22 nucleotides. The dysregulation of miRNA expression is often related to the development of various diseases, including human cancers (Calin et al., 2002). It also takes part as regulatory factors in a number of biological processes via repression of mRNA translation (Lu et al., 2005). Whether directly or indirectly, some microRNAs act as cancer suppressors while others act as oncogenes (Esquela-Kerscher et al., 2006). These findings highlight the significance of using microRNA as a tool to promote the diagnostic, prognostic and therapy research progress. Therefore, there are urgent demands for constructing sensitive and selective sensing methods for miRNA detection. Recently, various strategies, such as electrochemistry (Yang et al., 2014), fluorescence (Degliangeli et al., 2014; Wu et al., 2014), chemiluminescence (Deng et al., 2013a, 2013b), colorimetry (Zhou et al., 2015; Shen et al., 2013), backscattering interferometry (Adams et al., 2013), and mass spectrometry (Popova and Williamson, 2014), etc. have been proposed. Still, it is a challenge to explore new protocols and schemes for further improvement of their sensitivity or simplification. Meanwhile, it is of great value to explore a new strategy for determination of miRNA level in complicated biological mixtures (for example, in cell samples).

A quartz crystal microbalance (QCM) is a useful instrument to detect directly guest molecule binding processes by measuring mass changes induced frequency changes at a host monolayer (Höök et al., 1998). Besides, its low cost, real time output, and label-free entities also attracted researchers' interests (Cheng et al., 2012). QCM has been successfully used in various biological analyses to study interactions between biomolecules (Zhang et al., 2015; Takahashi et al., 2012; Patel et al., 2009), biomolecules and abiotic molecules (Tang et al., 2014; Nelson et al., 2015; Kim et al., 2015), because of the capability to monitor the interactions in a dynamic, label-free, and noninvasive way (Takahashi et al., 2009;

* Corresponding author.
E-mail address: xujj@nju.edu.cn (J.-J. Xu).

http://dx.doi.org/10.1016/j.bios.2016.06.013
0956-5663/

Uludag and Tothil, 2012). The assay is mainly implemented by detecting the frequency change before and after the target biomolecules reacted with the corresponding ligands immobilized on QCM surfaces, and the change is usually limited. Thus, QCM-based assay is suitable for high molecular weight targets. In that light, is there anything more beneficial to do facing lower molecular weight targets? Signal amplification of course must be considered as a good idea.

Dendrimers, a new class of repetitively branched macromolecules with a tree-like topological structure, are versatile candidates as scaffolds for cancer detection and therapy (Li et al., 2016; Myung et al., 2015). The peripheral functional groups existed on the surface predominantly determine the physicochemical properties of a dendrimer. Ju et al. (Deng et al., 2013b) designed a ferrocenyl-terminated dendrimer as an efficient tracing tag to quench the cathodic electrochemiluminescence emission in a sensitive bioanalysis strategy. Tsourkas et al. (Cheng et al., 2010) have demonstrated the utility of dendrimer nanoclusters as optical and MR imaging contrast agents for in vitro and in vivo detection of folate receptor over-expressed on tumor cells. Xu et al. prepared an Ag–PAMAM–luminol nanocomposite as a signal probe for the detection of cancer cells (Wang et al., 2016b).

Here, we modify amine-terminated dendrimers via coupling of their terminal amine groups to gold nanoparticle (GNP) surface, and utilize the modified dendrimer-surface to build bifunctional nanostructures which act as a signal probe in chemical and biological reactions. DNA (S1 or S2) is modified on GNP surfaces resulting in the formation of DNA/GNP/dendrimers. Through the complementary base pairing, DNA/GNP/dendrimers is captured on gold film chip followed by recording the changes of resonant frequencies (Δf). DNA/GNP/dendrimers can provide a larger surface coverage for the conjugation in comparison with DNA/GNP conjugates alone. Target microRNA could bind to a stem-loop-structured sequence (S3) on MNP, forming a heteroduplex. Only the DNA strand in this heteroduplex can be hydrolyzed by the enzyme duplex-specific nuclease (DSN), a linker sequence is left on MNPs and the released RNA molecule is back to hybridize another S3. The recycling amplification leads to a large number of linker sequences. Finally, Δf was obtained after complementary effect among capture sequence (S4), linker sequence and probe sequence (S1).

2. Experiments

2.1. Chemicals and materials

N-hydroxysuccinimide (NHS), 1-ethyl-3-(3-dimethylaminopropyl)-carbodiimide hydrochloride (EDC), Mercaptoacetic acid (MPA) and mercaptoethanol (MCH) were obtained from Aladdin. Polyamidoamine dendrimer (PAMAM, ethylenediamine core, generation 5.0) and chloroauric acid ($HAuCl_4$) were purchased from Sigma-Aldrich Chemical Co., Ltd. Duplex-specific nuclease (DSN, 50 U) was purchased from Evrogen Joint Stock Company (Russia). Avidin-magnetic nanoparticles were obtained from Tiandz (Beijing, China, ~100 nm). Homobifunctional, amine-reactive cross-linkers with polyethylene glycol (PEG) spacer arms $BS(PEG)_5$ (MW 532.50) was purchased from Pierce. All the DNA/RNA sequences were synthesized and purified by Sangon Biotech Co. Ltd. (Shanghai, China), and the sequences of this work are listed in Table S1. All other reagents were of analytical grade and used without further purification. Gold film chip was bought from Q-Sense.

2.2. Apparatus

Transmission electron microscopy (TEM) images were recorded using a JEM-2100 (Hitachi, Japan) instrument. Scanning electron microscopy (SEM) images were recorded using an S-3400 (Hitachi, Japan) instrument. QCM detection was performed on a Q-sense instrument (Q-Sense E1, Vastra Frolunda, Sweden). UV/Vis absorption spectra were obtained with a Cary 60 Series Spectrophotometer (Varian, Australia). Raman measurements were performed on a Renisaw Invia Raman spectrometer (RamLab-010). All glassware used in this work was thoroughly cleaned in aqua regia (3 parts HCl, 1 part HNO_3), rinsed in doubly distilled H_2O, and oven-dried prior to use.

2.3. Preparation of GNPs

Gold nanoparticles (GNPs) were prepared according to literature (Frens, 1973) with slight modification. 1 mM $HAuCl_4$ and 38.8 mM sodium citrate stock solutions were prepared with doubly distilled H_2O that had been filtered through a 0.8 μm membrane filter. Other solutions were made fresh as needed using doubly distilled, filtered H_2O. In a round-bottom flask equipped with a condenser, 500 mL of 1.0 mM $HAuCl_4$ was brought to a rolling boil with vigorous stirring. Rapid addition of 50 mL of 38.8 mM sodium citrate to the vortex of the solution resulted in a color change from pale yellow to burgundy. Boiling was continued for 10 min; the heating source was removed, and stirring was continued for another 20 min to form gold nanoparticals (GNPs). After the solution reached to room temperature, it was stored in a refrigerator at 4 °C.

2.4. Preparation of MPA-modified GNP

Mercaptoacetic acid (MPA)-modified GNP was prepared by ligand-exchange reaction between MPA and GNP. A 100 mL of the as-prepared gold colloid was mixed with a 100 μL of aqueous solution of 20 mM MPA under stirring. The mixed solution was stirred overnight under room temperature. Then the GNPs were washed by centrifugation and supernatant was discarded to remove the sodium citrate and excessive MPA. The MPA-GNP was then redispersed by water to give a total volume of 100 mL and stored at 4 °C.

2.5. Preparation of DNA/GNP/dendrimer probe

Scheme 1A shows the fabrication procedure of the DNA/GNP/dendrimer probe. According to the literature (Cheng et al., 2010), dendrimer nanoclusters were prepared as follows. 100 μL of 0.2 mM NHS-PEG-NHS as the homobifunctional amine-reactive cross-linking agent was mixed with 0.5 mg dendrimer nanocluster for 20 h. After multiple washes with centrifugal filter devices, uncross-linked dendrimers were removed. Cross-linked dendrimers were collected and re-dispersed in 1.0 mL PBS. 200 μL of 0.1 M EDC and 200 μL of 0.02 M NHS were added to 10 mL MPA-modified GNP for 4 h to activate GNPs. The activated GNPs were washed by centrifugation and supernatant was discarded. Then the activated GNPs were mixed with cross-linked dendrimers and reacted for 4 h to form GNP/dendrimer. Unlinked GNPs were removed by centrifugal filter devices. Then 200 μL of 1.0×10^{-5} M S2 (5′-NH_2-TTT TTT TTT-3′) and 200 μL of 1.0×10^{-6} M S1(5′-NH_2-TTT CCG TCG AGT-3′) were added to the GNP/dendrimer and incubated at 37 °C for 12 h, then unbound DNA was removed by centrifugation. The prepared DNA/GNP/dendrimer probe was stored in the refrigerator at 4 °C.

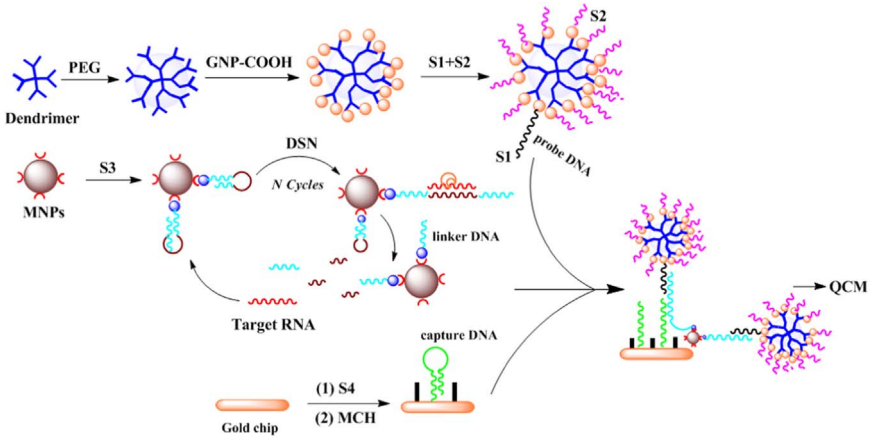

Scheme 1. Scheme of microRNA-mediated signal amplification coupled with GNP/dendrimers for microRNA detection.

2.6. Preparation of S4-modified gold film chips

Before modification with S4 (5′-ACG CTG AGC TTT TTT TTA CAG CGT-SH-3′), the gold film chip was immersed in piranha solution (98% H_2SO_4/30% H_2O_2=3/1, v/v) for 10 min, and rinsed thoroughly with doubly distilled water. Then the chip was immersed in a boiling solution (30% H_2O_2, 28% ammonia, and double distilled water in a volume ratio of 1:1:5) for 10 min. At last, the cleaned chip was rinsed thoroughly with doubly distilled water, and dried by nitrogen gas prior to use. 100 μL of 1.0 μM S4 was transferred on the chip above, and incubated at 25 °C overnight. Then 50 μL of 0.1 mM mercaptoethanol (MCH) was transferred on the chip for 1 h to block the uncovered chip. The modified chip was rinsed with doubly distilled water, and dried by nitrogen gas prior to use.

2.7. Preparation of mass-sensitive biosensor for the microRNA detection

200 μL of 1.0×10^{-6} M biotinylated S3 (5′-Bio-TTT GCT CAG CGT ACT CGA CGG CTA GTG GTC CTA AAC ATT TCA C CTG AGC-3′, 2-OMe-RNA are marked with underline) was reacted with 200 μL streptavidin-modified magnetic nanoparticles (MNPs) for 1 h. After being washed with PBS buffer through magnetically controlled separation, the resulting S3-MNPs were incubated in100 μL target microRNA solution in different concentrations, followed by adding 5 U DSN at 55 °C for 90 min. After the MNPs were washed twice, they were then injected on S4 modified-chip surfaces at room temperature to allow binding interactions. Next, the biosensor surface was washed by injection of PBS and water successively in preparation for performing sandwich assays. And then, DNA/GNP/dendrimer probe was injected on the biosensor surface. The frequency changes were recorded all through the injection processes.

2.8. Preparation of cellular extracts

The cellular extracts were prepared according to the reported method with minor modification (Osborn et al., 1989). Briefly, 2×10^7 cells were washed three times and suspended in 20 μL PBS buffer. After incubating for 15 min on ice, the lysed cellular suspension was briefly mixed on a vortex and centrifugated for 15 min at 4 °C. Then the supernatant was diluted to 80 μL and stored at −80 °C.

3. Results and discussion

3.1. The principle of strategy

The strategy comprised an enzymatic amplification process and a dendrimer enhancing process (Scheme 1). The enzymatic amplification process presented was based on the unique selectivity of DSN, which specifically cleaved double-stranded DNA (dsDNA) and DNA in DNA-RNA hybrid duplexes. (Degliangeli et al., 2014; Qiu et al., 2015; Wang et al., 2016a, 2016b; Lin et al., 2013) The biotin tag on stem-loop-structured sequence (S3) could bind specifically to magnetic nanoparticles (MNPs)-conjugated avidin. The S3 bound to its RNA complement to form the hybrid. The enzyme DSN could be capable of specifically cleaving only the DNA strand in this hybrid, then releasing the stem part (linker sequence). This RNA molecule can then bind to another S3, causing the cleavage of a second S3. This cyclic process results in an amplification effect whereby a very small amount of RNA molecules can release a lot of linker DNA on MNP. Thiolated DNA (S4) was directly anchored to gold film chip via the Au-S chemistry. Via the combination of probe DNA, the linker DNA on MPP and a capture DNA on gold chip, the DNA/GNP/dendrimer probe could be assembled on the surface of gold chip inducing a sensitive frequency response. SEM images of gold chip surface before and after bound with dendrimers were shown in Fig. S1. Figs. S2 shows the TEMs of the initial dendrimer (A), cross-linked dendrimer (B) and GNP/dendrimer (C). We can see that cross-linking induces the size of the dendrimers increase and many GNPs with the size of ~10 nm could be conjugated on the dendrimers. Here microRNA-203 was used as a model for detection. To demonstrate the feasibility of the strategy, polyacrylamide gel electrophoresis was performed. As illustrated in Fig. 1, the complex of S1/S3 could not be formed when S1 was incubated with S3 (line 4) and the complex of S4/part of S3 also could not be formed without microRNA-203 and DSN (line 5). When there were microRNA-203, S1, S3, S4 and DSN at the same time, the complex of S4/part of S3/S1 hybridized (line 8).

The quartz crystal microbalance (QCM) can quantify directly the mass adsorbed (Δm) on the sensor surface for a given change in resonance frequency (Δf) of the crystal: $\Delta m = -(C_{QCM}/n)/\Delta f$. C_{QCM} is the crystal-specific mass sensitivity constant and n is the overtone number. Frequency shift of QCM sensors is indicative of changes in mass character of the detection media (Chen et al., 2011). A downward shift in resonance frequency is still accepted as a good indication of added mass, while upward shift indicates of reduced mass (Knudsen et al., 2006). S3 was modified with 2-OMe on its stem, which differs from DNA in the 2-OMe on the pentose.

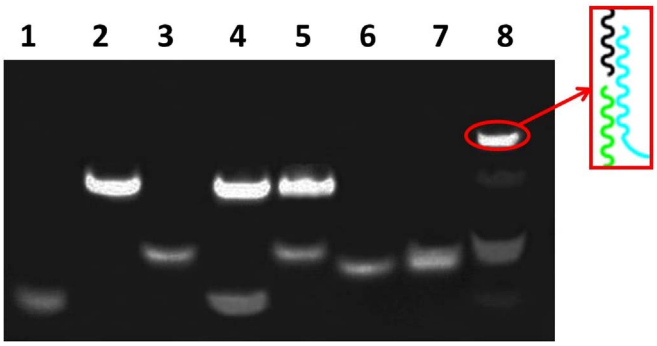

Fig. 1. Agarose gel electrophoresis image for hybridization protection assay: line 1, S1; line 2, S3; line 3, S4; line 4, S1+S3; line 5, S3+S4+DSN; line 6, microRNA-203; line 7, microRNA-203+S4+DSN; line 8, microRNA-203+S1+S3+S4+DSN.

S3 will not be recognized and cleaved by DSN (Lin et al., 2013). To investigate the cleavage by DSN, unmodified S3′ was used as a control test. Biotinylated S3 or S3′ was attached with MNPs. S3-MNPs or S3′-MNPs were incubated in target microRNA solution or target microRNA+DSN solution. After washed twice, the solutions were then injected on S4 modified-chip surfaces at room temperature to allow binding interactions. Then, DNA/GNP/dendrimer probe was injected on the biosensor surface. The frequency changes were recorded during the injection processes. As shown in Fig. 2A, line 1 and line 3 presented S3 and S3′ respectively. S3 was not vulnerable towards hydrolysis by DSN (line 2). After interaction with DSN, S3′ was vulnerable towards hydrolysis by DSN (line 4). Frequency measurements were obtained to study the cleavage by DSN. As can be seen from Fig. 2B, the obvious frequency change was only occurred when S3 was incubated with DSN. When we used S3′ instead of S3, the frequency is same as those without DSN, indicating S3′ was cleaved by DSN. These results confirmed that S3 was protected from hydrolysis by DSN.

To investigate the amplification and enhancement effect, incubation experiments of capture S4 hybridized with linker DNA in the presence or absence of "DSN or DNA/GNP/dendrimer probe" were carried out. As shown in Fig. 3, after DSN enzymatic amplification process, the linker sequence was captured by S4 and the frequency was reduced (curve a). And then DNA/GNP/dendrimer probe was linked on gold film chip. The frequency was significantly reduced due to the increase of mass (curve a). But no significant signal change (curve c) was observed in the absence of

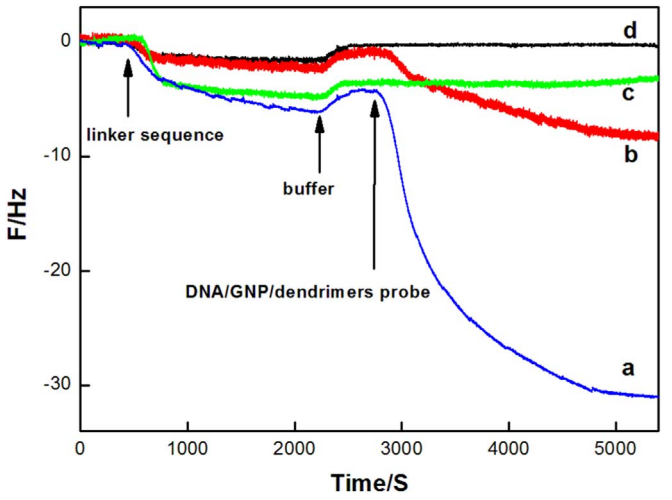

Fig. 3. The f-responses assay with 1.0×10^{-10} M microRNA-203. Curve a: in the presence of both DSN and DNA/GNP/dendrimer probe; curve b: in the presence of only DNA/GNP/dendrimer probe; curve c: in the presence of only DSN; curve d: in the absence of both DSN and in DNA/GNP/dendrimer probe.

"DNA/GNP/dendrimers probe". In the absence of DSN and DNA/GNP/dendrimers probe (curve d), linker sequence couldn't induce Δf-response. In the presence of DNA/GNP/dendrimer probe without DSN (curve b), Δf-response showed slight change because of some nonspecific adsorption. The frequency response in the presence of both DSN and DNA/GNP/dendrimer probe was approximately 3.6-fold that in the presence of only DNA/GNP/dendrimer probe and approximately 12-fold that in the presence of only DSN. Those results indicated that the amplification and enhancement processes acted superimposed effect for target detection.

To further prove the principle of strategy, a series of Raman experiments were performed with roxithromycin (ROX, as Raman signal probe) modified S2 on 3′ end (named as S2′) replacing S2 (Scheme S1). The results are shown in Fig. S3. Only in the presence of both target RNA and S2′, Raman signal could be observed and the signal increased as microRNA-203 concentration increased correspondingly, confirming the process in Scheme 1.

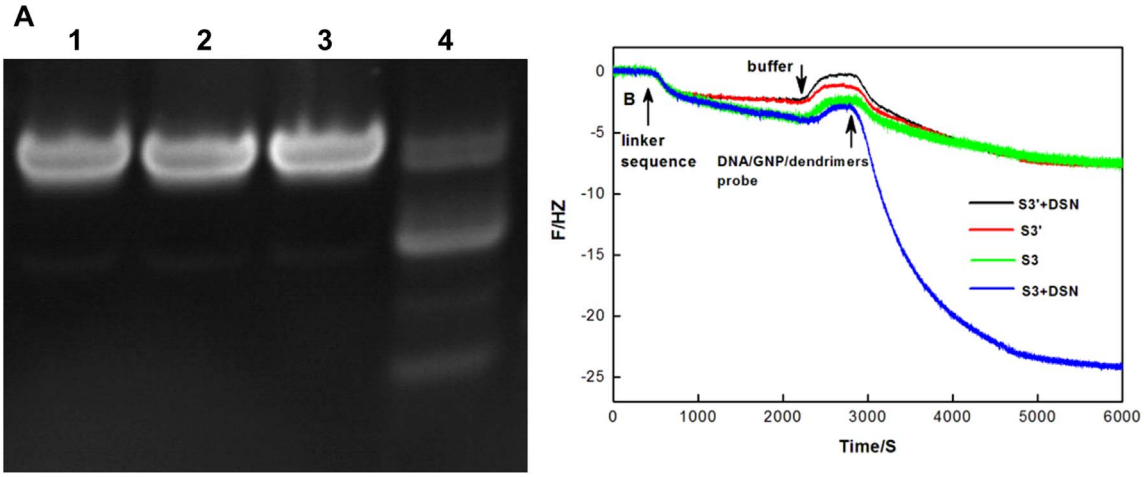

Fig. 2. (A) agarose gel electrophoresis image for hybridization protection assay: line 1, S3; line 2, S3+DSN; line 3, S3′; line 4, S3′+DSN. (B) f-responses assay: S4 was directly anchored to gold film chip. Black: S3′ bind specifically to MNPs and DSN was added to the solution. Red: S3′ bind specifically to MNPs and no DSN was added to the solution. Green: S3 bind specifically to MNPs and no DSN was added to the solution. Blue: S3 bind specifically to MNPs and DSN was added to the solution. (For interpretation of the references to color in this figure legend, the reader is referred to the web version of this article.)

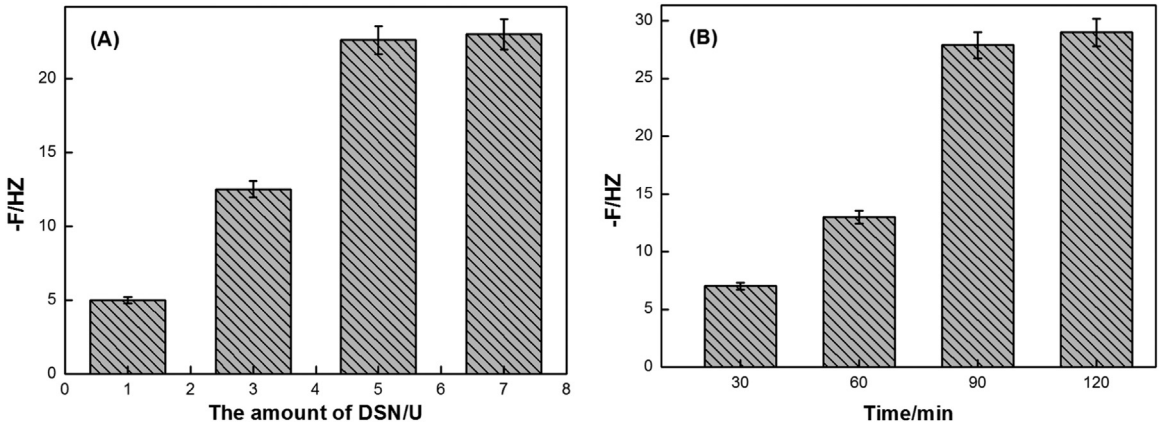

Fig. 4. (A) The frequency responses on the amount of DSN (microRNA-203: 1.0×10^{-10} M; the enzymatic amplification process time: 80 min); (B) The frequency responses on the enzymatic amplification process time (microRNA-203: 1.0×10^{-10} M; DSN: 5 U).

3.2. The Sensitivity

To obtain the good sensitivity, we investigated the effect of the amount of DSN and the time of enzymatic amplification process on the frequency responses. As shown in Fig. 4A, the fluorescence intensity increased rapidly with the increase of the DSN amount at first and reached an equilibration step at the amount of 5 U. Thus, this concentration was selected for the subsequent assays. As shown in Fig. 4B, the frequency increased with the enzymatic amplification process and reached a plateau at 90 min. When the time was more than 90 min, the frequency did not show obvious change. Therefore, the enzymatic amplification reaction time was controlled at 90 min all through the experiment. Compared with methods reported by literature (Wang et al., 2016a, 2016b), advantages of the present method is the rapid reaction rate.

The frequency changes upon addition of target microRNA-203 at different concentrations were measured. As shown in Fig. 5A, the frequency significantly decreased with the concentration of target microRNA-203 increasing from 1.0×10^{-12} M to 1.0×10^{-9} M. As the concentration of target microRNA-203 increases, the formation of enzyme cleavage is enhanced, implying an increased content of the linker sequence on MNP and the hybridized sandwich composite. The standard calibration curve for microRNA-203 detection is shown in the inset of Fig. 5B. The linear range of the response versus the log [microRNA-203] was 1.0×10^{-11}–1.0×10^{-9} M. The detection limit was 1.0×10^{-12} M, which was lower than the polydopamine-based method for microRNA detection coupling DSN-aided target recycling strategy (Wang et al., 2016a, 2016b). The regression equation could be expressed as Y=21.4X+238.3 (Y represents the change of QCM frequency; X represents the logarithm of microRNA-203 concentration, M; R=0.99). According to the linear equation, we could detect microRNA concentration quantitatively. Such a low level of detection of microRNA-203 due to the significant signal amplification and enhancement by the DSN and DNA/GNP/dendrimer probe is comparable with previously reported methods.

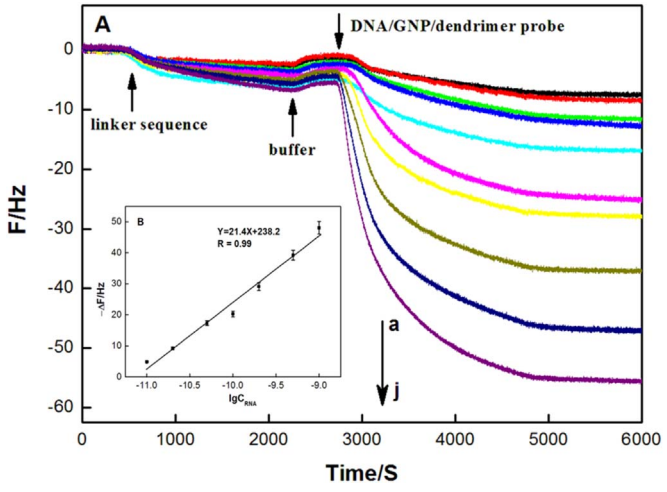

Fig. 5. (A) Time-dependent frequency responses with different target microRNA-203 concentrations (a-j: 0, 1.0×10^{-12}, 5.0×10^{-12}, 1.0×10^{-11}, 2.0×10^{-11}, 5.0×10^{-11}, 1.0×10^{-10}, 2.0×10^{-10}, 5.0×10^{-10}, 1.0×10^{-9} M); (B) a calibration plot of saturated frequency shift versus microRNA-203 concentration.

3.3. The selectivity

To examine the selectivity of this assay to specific miRNA detection, we conducted a comparison study on various noncomplementary and mismatched targets from perfect complementary targets. Different kinds of targets including the perfect complementary target (c) and two-base-mismatched (mc) and unrelated (nc) target sequences were chosen at three concentrations (1.0×10^{-12} M, 1.0×10^{-10} M, 1.0×10^{-9} M). Fig. S4 shows the differences of frequency responses obtained from different solutions of noncomplementary and mismatched miRNA. As expected, it was observed that only the complementary target microRNA-203 gave the significant change in frequency. In contrast, the frequency changes triggered by mismatched targets were very small. This is due to the intrinsic property of DSN, which has the capability to discriminate between the perfectly and non-perfectly matched short DNA-RNA hybrid duplexes with a nucleotide mismatch (Shagin et al., 2002). The significant difference between perfect-matched and mismatched targets indicates that our method readily discriminates between matched and mismatched microRNA with high specificity. The proposed method was compared with other DSN-based detection methods and the results were summarized in Table S2. These data indicate that the proposed method has potential to detect biological samples.

3.4. The feasibility in cell lysate

To evaluate the feasibility of our proposed method in real biological samples, the concentrations of microRNA-203 in cell lysate were obtained by employing a standard curve method. The concentrations of microRNA-203 spiked were plotted against Δf response. The determined microRNA-203 concentration was 309 copies/cell ($\sim 2.91 \times 10^{-10}$ M). The value of microRNA-203 quantified by the proposed platform was compared with the outcome of a commercial qRT-PCR method (575 copys/cell). The high

correlation with the commercial qRT-PCR method demonstrated that our method could be used for microRNA quantification in cell lysate samples. We also determined the accuracy of the method by measuring the recovery of different concentrations of microRNA-203 spiked into the cell lysates (Table S3 in the Supplementary material). The method reveals good recovery rates of standard addition from 97% to 105%. These results indicated that the proposed method was capable of detecting miRNA sensitively in real complex samples.

4. Conclusion

In conclusion, a mass-sensitive biosensor based on microRNA-mediated signal amplification coupled with GNP/dendrimer-induced signal enhancement was developed. It presented good performance on its applications in intracellular microRNA quantification. Both the success in discriminating expressing miroRNA-203 in MCF-7 cell and the well agreement with the commercial qRT-PCR detection method justified the proposed system in application for future early cancer diagnosis.

Acknowledgement

This work was supported by the National Natural Science Foundation of China (21575056, 21135003 and 21305059), the Program for New Century Excellent Talents in University of Ministry of Education of China (NCET-13-0845), the Project for Science Apparatus Improvement of Shandong Province (2013SJGZ25), the Project of Shandong Province Higher Educational Science and Technology Program (J13LD19) and the China Postdoctoral Science Foundation (2014M551549).

Appendix A. Supplementary material

Supplementary data associated with this article can be found in the online version at http://dx.doi.org/10.1016/j.bios.2016.06.013.

References

Adams, N.M., Olmsted, I.R., Haselton, F.R., Bornhop, D.J., Wright, D.W., 2013. Nucleic Acids Res. 41, e103.
Calin, G.A., Dumitru, C.D., Shimizu, M., Bichi, R., Zupo, S., Noch, E., Aldler, H., Rattan, S., Keating, M., Rai, K., Rassenti, L., Kipps, T., Negrini, M., Bullrich, F., Croce, C.M., 2002. Proc. Natl. Acad. Sci. USA 99, 15524–15529.
Chen, J.Y., Li, M.H., Penn, L.S., Xi, J., 2011. Anal. Chem. 83, 3141–3146.
Cheng, C.I., Chang, Y.P., Chu, Y.H., 2012. Chem. Soc. Rev. 41, 1947–1971.
Cheng, Z.L., Thorek, D.L.J., Tsourkas, A., 2010. Angew. Chem. Int. Ed. 49, 346–350.
Degliangeli, F., Kshirsagar, P., Brunetti, V., Pompa, P.P., Fiammengo, R., 2014. J. Am. Chem. Soc. 136, 2264–2267.
Deng, H.M., Ren, Y.Q., Shen, W., Gao, Z.Q., 2013a. Chem. Commun. 49, 9401–9403.
Deng, S.Y., Lei, J.P., Liu, Y., Huang, Y., Ju, H.X., 2013b. Chem. Commun. 49, 2106–2108.
Esquela-Kerscher, A., Slack, F.J., 2006. Nat. Rev. Cancer 6, 259–269.
Frens, G., 1973. Nature 241, 20–22.
Höök, F., Rodahl, M., Kasemo, B., Brzezinski, P., 1998. Proc. Natl. Acad. Sci. USA 95, 12271–12276.
Kim, S.S., Kuang, Z.F., Ngo, Y.H., Farmer, B.L., Naik, R.R., 2015. ACS Appl. Mater. Interfaces 7 (36), 20447–20453.
Knudsen, S.M., Lee, J., Ellington, A.D., Savran, C.A., 2006. J. Am. Chem. Soc. 128, 15936–15937.
Li, T.Y., Smet, M., Dehaen, W., Xu, H.P., 2016. ACS Appl. Mater. Interfaces . http://dx.doi.org/10.1021/acsami.5b07877.
Lin, X.Y., Zhang, C., Huang, Y.S., Zhu, Z., Chen, X., Yang, C.J., 2013. Chem. Commun. 49, 7243–7245.
Lu, J., Getz, G., Miska, E.A., Alvarez-Saavedra, E., Lamb, J., Peck, D., Sweet-Cordero, A., Ebert, Benjamin, L.R., Mak, H., Ferrando, A.A., Downing, J.R., Jacks, T., Horvitz, H. R., Golub, T.R., 2005. Nature 435, 834–838.
Myung, J.H., Roengvoraphoj, M., Tam, K.A., Ma, T., Memoli, V.A., Dmitrovsky, E., Freemantle, S.J., Hong, S., 2015. Anal. Chem. 87, 10096–10102.
Nelson, G.W., Parker, E.M., Singh, K., Blanford, C.F., Moloney, M.G., Foord, J.S., 2015. Langmuir 31, 11086–11096.
Osborn, L., Kunkel, S., Nabel, G.J., 1989. Proc. Natl. Acad. Sci. USA 86, 2336–2340.
Patel, A.R., Kanazawa, K.K., Frank, C.W., 2009. Anal. Chem. 81, 6021–6029.
Popova, A.M., Williamson, J.R., 2014. J. Am. Chem. Soc. 136, 2058–2069.
Qiu, X., Liu, X., Zhang, W., Zhang, H., Jiang, T., Fan, D., Luo, Y., 2015. Anal. Chem. 87, 6303–6310.
Shagin, D.A., Rebrikov, D.V., Kozhemyako, V.B., Altshuler, I.M., Shcheglov, A.S., Zhulidov, P.A., Bogdanova, E.A., Staroverov, D.B., Rasskazov, V.A., Lukyanov, S., 2002. Genome Res. 12, 1935–1942.
Shen, W., Deng, H.M., Ren, Y.Q., Gao, Z.Q., 2013. Chem. Commun. 49, 4959–4961.
Takahashi, S., Tsuji, K., Ueda, T., Okahata, Y., 2012. J. Am. Chem. Soc. 134, 6793–6800.
Takahashi, S., Iida, M., Furusawa, H., Shimizu, Y., Ueda, T., Okahata, Y., 2009. J. Am. Chem. Soc. 131, 9326–9332.
Tang, W., Policastro, G.M., Hua, G., Guo, K., Zhou, J.J., Wesdemiotis, C., Doll, G.L., Becker, M.L., 2014. J. Am. Chem. Soc. 136 (46), 16357–16367.
Uludag, Y., Tothill, I.E., 2012. Anal. Chem. 84 (14), 5898–5904.
Wang, Q., Yin, B.C., Ye, B.C., 2016a. Biosens. Bioelectron. 80, 366–372.
Wang, Y.Z., Hao, N., Feng, Q.M., Shi, H.W., Xu, J.J., Chen, H.Y., 2016b. Biosens. Bioelectron. 77, 76–82.
Wu, P., Tu, Y.Q., Qian, Y.D., Zhang, H., Cai, C.X., 2014. Chem. Commun. 50, 1012–1014.
Yang, C.Y., Dou, B., Shi, K., Chai, Y.Q., Xiang, Y., Yuan, R., 2014. Anal. Chem. 86, 11913–11918.
Zhang, S.L., Bai, H.H., Pi, J., Yang, P.H., Cai, J.Y., 2015. Anal. Chem. 87, 4797–4805.
Zhou, W.J., Liang, W.B., Li, X., Chai, Y.Q., Yuan, R., Xiang, Y., 2015. Nanoscale 7, 9055–9061.